# ALPI super-conducting accelerator

# 1

The ALPI project started in 1989 with the primary goal of extending the XTU TANDEM performance toward heavier beams and higher energies due to the demands of nuclear physics experiments. Since the very beginning the project adopted the philosophy of basing the acceleration on independently phased super-conducting quarter wave resonators (QWR) and following the Argonne National Laboratories it carried out the idea of installing a positive ion injector (PIAVE) in order to substantially improve the beam intensity of medium-heavy ion species. In 1995 the first beams were successfully accelerated and from that time on the accelerator has provided thousand hours of stable operation.

Since January 2006 the ALPI acceleration set-up has been based on beam dynamics simulations which have given the opportunity of speeding up the beam preparation time and of a better understanding of the machine.

## 1.1 ALPI: a brief description

The ALPI project [1], funded in 1989, was divided in two phases. The first phase was intended to allow the acceleration of the intermediate ion mass range, from Si up to I, and it was based on 160 MHz OFHC Copper lead plated Quarter Wave Resonators (QWR) with an optimum velocity of $\beta_o = 0.11$. The second phase foresaw to extend the acceleration to higher masses with the use of bulk Niobium resonators $\beta_o = 0.055$ operating at 80 MHz. This phase was conducted in parallel with the design of the new positive injector PIAVE. In the meantime the plating technology had evolved and it was possible to replace the Lead-on-Copper cavities with the far better performing Niobium-on-Copper ones. At the present the accelerator is comprised of 3 cryostats of low-β cavities, 11 of medium-β and 2 of high-β ($\beta_o = 0.13$) for a total voltage of 48 MV and 64 QWRs.

In order to use the existing experimental halls, ALPI was folded in two parallel lines (low- and high-energy branch) connected with a U-bend (see Fig. 1.1). Two long connection lines were built to inject the beam from the TANDEM and to bring the beam back to the experimental halls. The magnetic lattice contains two 90° dipoles, which bend the beam coming from the TANDEM into the low-energy branch, four 45° dipoles, for the U-bend, and two more 45° dipoles to bend rightward to return to the experimental halls.

In order to simplify the shielding of the machine, ALPI is placed 4 m below the TANDEM level. To overcome this displacement the two 90° magnets are tilted by an angle of −7° and in the return line there are two 6° vertical dipoles that bring back the beam to the level of the TANDEM vault. To complete the machine there are 3 quadrupole doublets and 23 triplets providing proper transverse focussing and 6 singlets to make all the bendings isochronous and achromatic.

The basic unit of the machine is the module, made of two cryostats, one triplet and a diagnostic box (see Fig. 1.2). Every module contains a diagnostic box which can monitor the two transverse planes profiles and the beam current intensity. Other diagnostic boxes are placed along the injection and extraction line that allow to check the beam transport at every beam waist.

The transverse plane detectors are Beam Profile Monitors made of two grids of 39 thin

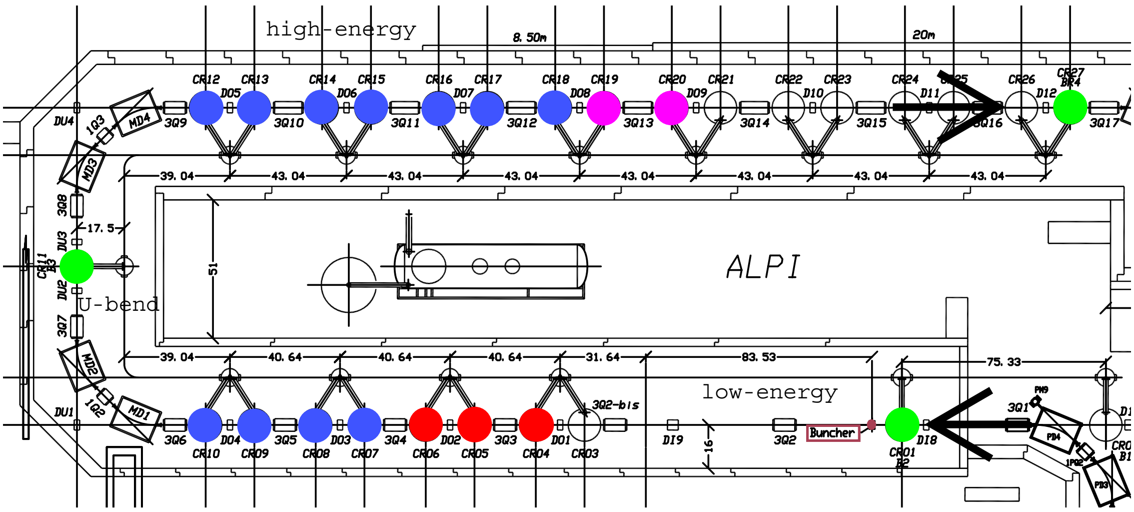


Figure 1.1: ALPI layout. The beam coming from either PIAVE or TANDEM injector is accelerated by the low-β (in red), medium-β (blue) and high-β (magenta) cryostats. Each cryostat houses 4 Quarter Wave Resonator (QWR). The accelerator is divided in three zones, the so called low-energy branch, the U-bend and the high-energy branch. The first green cryostat (1 QWR) is used to bunch the beams injected by the TANDEM, the second one (2 QWRs) to rebunch the beam between the two branches and the last one (1 QWR) as energy spread suppressor.

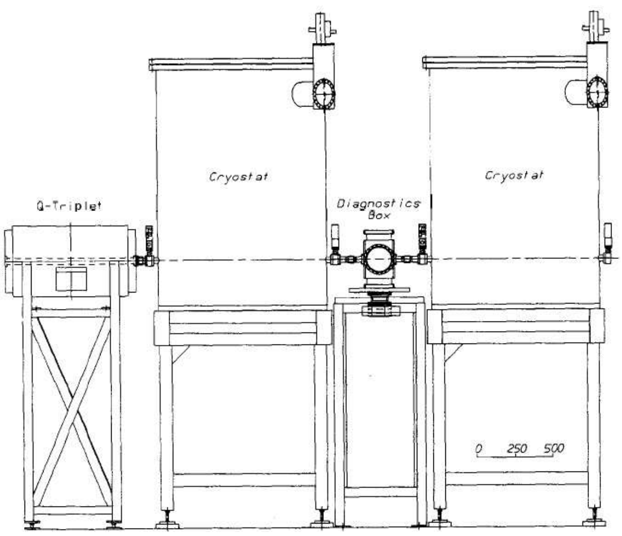


Figure 1.2: Basic module of the linac. The diagnostics box houses a Faraday Cup to measure the beam current and two grids to record beam centroid and width. Since the grids intercept only 10% of the beam, it is possible to set the transverse optics (tune the magnets) looking at the result in real time.

tungsten-rhenium wires, 20 μm in diameter and a pitch of 250 μm which give a beam transmission of the order of 90%. The diagnostics workstations control both the BPM and the Faraday cup and show on the same display the value of the current and the horizontal and vertical profiles.

## 1.2 ALPI cavity performances

ALPI was proposed in the late 80's as the INFN-LNL super-conducting booster. At that time it was decided that the electroplating of a Pb superconductor layer onto a Cu substrate would be the "working horse" technology for the first period of the linac operation. The plan foresaw the construction of 95 Nb Pb/Cu resonators [2], with a target accelerating field of 3 MV/m (corresponding to a peak surface field $E_{s,p} \sim 15$ MV/m), indeed a rather optimistic value, to achieve a final beam energy in the range $6 \div 20$ MeV/A (from the heavier nuclei like $^{90}$Zr to the lighter ones, such as $^{12}$C). These resonators would be contained in 27 cryostats, including 3 couples of buncher resonators.

### 1.2.1 Copper based resonators

The Pb/Cu electroplating technology was validated in 1990, when the first Q-vs-$E_{acc}$ tests showed that an accelerating field in the range $2.3 \div 2.7$ MV/m was achieved on a series of tests [3]. The construction of these resonators was carried out, together with the construction and assembly of the entire accelerator, in the following 4 years. Operation started in 1992 with 16 resonators (including 4 bunching units) and the installation of additional units followed (28 in 1993 and 4 in 1994). Pb/Cu resonators proved to be reliable for accelerator operation for a number of years. In particular, their excellent mechanical stability made it very easy to lock them in amplitude and phase to their reference values; moreover, the high thermal conductivity of Cu made them less susceptible to quench with respect to full Nb resonators.

On the other hand, however, their performance was rather limited, since their accelerating field rarely exceeded 3 MV/m (the specified value), averaging at about 2.6 MV/m as an operational number, reduced to 2.4 MV/m after a couple of years. Moreover, the handling of these cavities was somewhat complicated by the fact that the electroplated Pb surface was particularly prone to degradation when accidentally exposed to air, therefore a strict handling of Pb-plated resonators in a N atmosphere was mandatory at all times.

Aiming at a possible upgrade of the resonators accelerating voltage, since the very beginning of the ALPI project two R&D programmes were launched, one on the sputtering of Cu bases with Nb and the other on the realization of full Nb cavities. These programmes proceeded in parallel, reaching in the same year (1993), the outstanding result of an accelerating field of ~ 6 MV/m. At that time the construction of ALPI medium-β section (first ALPI construction phase) with Pb/Cu resonators was already nearly completed and the construction technology could not be changed. Given the success of the R&D phases, it was decided nevertheless to continue investing in both the Nb-sputtered and full-Nb technologies and, in the second phase of ALPI, to build the higher β section with the former and the lower β section with the latter.

#### High beta Nb/Cu resonators

The QWR Cu bases for the Nb sputtering technology were soon shaped in a geometry which would be best suited for the deposition of a Nb layer of uniform thickness. By means of some new design details, along with a careful and long setup of the delicate sputtering procedure, the first results were confirmed and exceeded in a number of tests, showing an average accelerating field off-line $E_{acc}$ $6 \div 8$ MV/m at $P_d = 7$ W (with $Q_0 \sim 6 \div 7 \times 10^8$ at the high field values) [7].

The technology was clearly mature to be applied to on-line resonators. It must be noted that their operation, despite the higher field, was indeed very similar to that of Pb/Cu resonators. The thick Cu base makes them in fact particularly stable to both mechanical vibrations and changes of the liquid He pressure ($P_{He}$). The sensitivity of the Cu-based resonator frequency to variations of

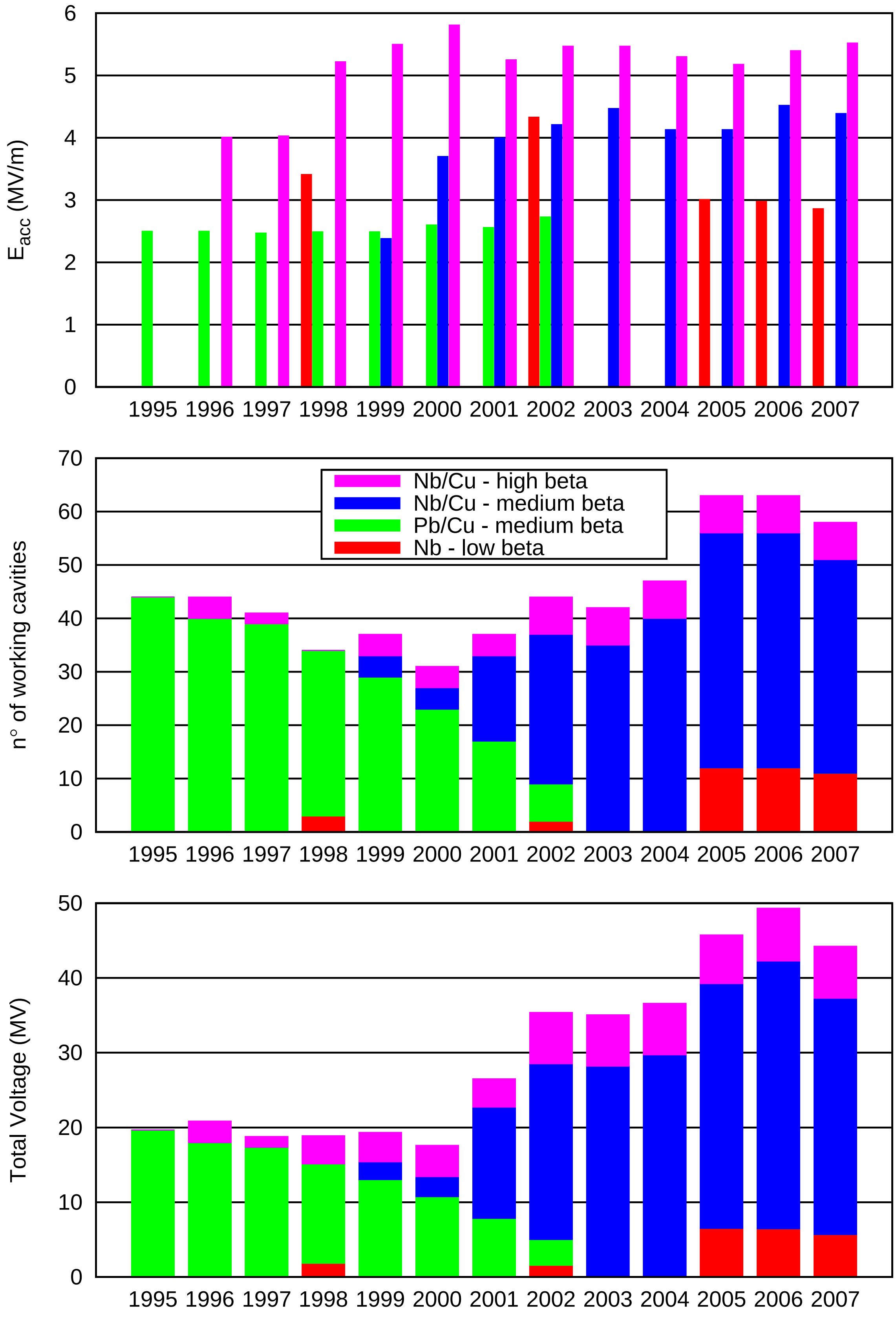


Figure 1.3: ALPI QWR performances since 1995.

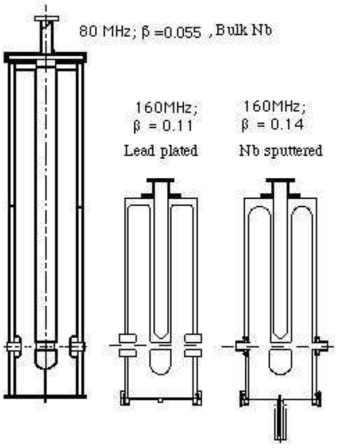


Figure 1.4: QWR structure comparison.

$P_{He}$ is as low as $\Delta f / \Delta P_{He} \sim 0.01$ Hz/mbar. Even large variations of $P_{He}$, which in ALPI can change even at a rate of 100 mbar/min, reflect in a rate of frequency variations in the order of 1 Hz/min, so small a value that it does not even need to be controlled via the mechanical tuners.

**Medium beta Nb/Cu resonators**

The success of the development of higher $\beta_o$ cavities opened the possibility to apply the sputtering technique to the medium-β section as well. With the aim of a cheap and quick process, sputtering of the same Cu bases which had been previously Pb-electroplated was attempted. The impulse to the medium-β resonator upgrade was given by a serious problem which started affecting a large number of cryostats in a close sequence: the leaking of a cryogenic valve, actuated by cold He gas in the common vacuum of the cryostat. A maintenance team was setup, with the main objective of fixing the problem of the leaking cryostats. At the same time, the old Pb/Cu cavities were upgraded with a newly sputtered Nb film. This process, being conducted with a schedule which should have no interference with the approved physics programme of the LNL facilities, lasted from 1999 to 2003, when the latest medium beta cryostat with mid-β resonators was upgraded.

In spite of the less favorable geometry (presence of beam ports, large radii on these and on the shorting plate, holes in the high current density region), the average accelerating field obtained increased by more than 60% (from 2.7 to 4.4 MV/m) [4]. It is noted, incidentally, that cryostats CRB3 and CRB4 (containing bunching resonators) still contain Pb/Cu cavities, which should be replaced in a near future.

The noteworthy success of the medium-β resonator upgrade triggered an R&D program, aimed at a further increase of the accelerating field of these resonators to be obtained by optimization of the shape of the Cu bases. At present 4 new resonators, with $\beta_o = 0.11$, are being fabricated and sputtered (fig.3). The first prototype was tested in July 2007 at 4 K [5]. At present the Q-vs-$E_{acc}$ curve cannot exceed 3 MV/m (radioprotection authorization limit), however the curve shape, together with previous experience, let an operational field $E_{acc} \sim 5.5$MV/m be extrapolated.

## 1.2.2 Niobium-based resonators

The development of full Nb QWRs started in 1987, with the construction of prototypes of 80, 160 and 240 MHz resonators till 1993. Then the production of 12 80 MHz $\beta_o = 0.055$ cavities began [6] and a first cryostat was installed in 1995. Lower $\beta_o$ cavities are required by beams injected from the Tandem and with A>80 and by beams injected by PIAVE (the last cavities of which have a $\beta_o$ value of 0.047).

By 1998 12 such resonators had been installed in ALPI [7]. Their average $E_{acc}$ at $P_c = 7$ W is around 7 MV/m: the higher resonator performance, with respect to the specified 3 MV/m, allowed installing 12, out of the originally foreseen 20, such resonators. Since their very first

Table 1.1: Combination of synchronous phases for a stable ALPI period (A/q = 7, $\beta$ = $\beta_o$ = 0.055).

| cryostat | | | | cryostat | | | | max $E_{acc}$ (MV/m) |
|---|---|---|---|---|---|---|---|---|
| -20 | -20 | -20 | -20 | -20 | -20 | -20 | -20 | 3.2 |
| +20 | -20 | -20 | -20 | -20 | -20 | -20 | +20 | 4.0 |
| -20 | +20 | -20 | -20 | -20 | -20 | +20 | -20 | 5.3 |
| -20 | -20 | +20 | -20 | -20 | +20 | -20 | -20 | 5.5 |
| -20 | -20 | -20 | +20 | +20 | -20 | -20 | -20 | 4.2 |
| +20 | -20 | -20 | -20 | +20 | -20 | -20 | -20 | 5.3 |
| -20 | +20 | -20 | -20 | +20 | -20 | -20 | -20 | 5.1 |
| -20 | -20 | +20 | -20 | +20 | -20 | -20 | -20 | 4.7 |
| +20 | -20 | -20 | -20 | -20 | +20 | -20 | -20 | 5.0 |
| -20 | +20 | -20 | -20 | -20 | +20 | -20 | -20 | 6.0 |
| +20 | -20 | -20 | -20 | -20 | -20 | +20 | -20 | 4.6 |

installation in 1995, ALPI QWRs have encountered a serious cryogenic problem. Thelayout of the ALPI cryogenic lines caused inefficient cooling of the cryostat thermal shields (provided by 7 bar He gas). Consequently, in the lower β branch of ALPI the shields temperature exceeded 100 K on the far end cryostats. The anomalous evaporation of liquid He in the cryostat dewar stopped the liquid He transfer. Therefore lower β cryostats (CR04-06) could never be efficiently refrigerated while the rest of ALPI was kept cold (with a couple of exceptions such as a single lower β cryostat cooled for very short beam times).

Only in 2004 a long maintenance shutdown of ALPI was planned, in order to perform a complete reshaping of cryogenic lines layout: by implementing the condition of constant pressure drop on each cryostat, the distribution of the shields temperature was far better balanced all along the linac [8]. As a result, the cryogenic operation of cryostats CR04-06 is working successfully since 2005.

## 1.3 Analysis of ALPI period

As said before, ALPI module is made by two cryostats and a magnetic triplet. In the low-energy branch the period length is 4.064 m whereas in the high energy is 4.300 m, because of the larger effective length of the triplets which are chosen for a higher beam rigidity. The cavities are placed inside the cryostat each 24 cm and, since the distance between the cryostats is 60 cm, it results that the cavities are closer to the period center than to the ends.

The main problem of having a longitudinal well matched beam all along the accelerator is that, if every cavity is operated at maximum $E_{acc}$, the cavity focusing force in linear approximation

$$k_z = \frac{2\pi \cdot E_{acc} \cdot L_{eff} \cdot TTF \cdot \sin\phi_s}{m_0 \cdot c^2 \cdot \beta^3 \cdot \lambda} \frac{q}{A}$$

is a function of the Transit Time Faction and the relativistic $\beta$. To have a smoothly varying or constant phase advance $\sigma_l$, the $E_{acc}$ should be tuned along the accelerator. This would imply that for low $\beta$ the $E_{acc}$ has to be reduced and for high $\beta$ enhanced, which would lower the average accelerating field. It means that more cavities are needed to reach the same energy.

The problem is complicated by the fact that two frequencies are present, 80 MHz in the low-β and 160 MHz in the medium-β, that would imply that one can obtain the matching between the sections only if the medium-β cavities work at half of the field of the low-β ones.

Analyzing the stability condition ($\sigma_l < \pi$) of the low-β period with $\phi_s = -20$ it results that the maximum $E_{acc}$ for A/q = 7 and $\beta = \beta_o = 0.055$ is 3.2 MV/m. The value scales as A/q, which means that for A/q = 4 the accelerating field would be 1.9 MV/m. The only way to reduce the phase advance is the use of positive synchronous phases. Using +20 in one of the cavities moves the limit to 3.3 MV/m, in both the cavities facing the triplets 4 MV/m. All the combination of synchronous phases are shown in Tab. 1.1.

For the medium-$\beta$ period, the -20 solution is stable at 4 MV/m starting from $\beta = 0.075$, implying that an energy at transition greater than 2.7 MeV/A is required to use the medium-$\beta$ cavities at full $E_{acc}$.

Not every combination is yet suitable for the transverse plane, since the the RF (de-)focusing acts in first approximation proportionally to the dimensions of the beam: a period where the positive synchronous phases are located close to the center will need a higher gradient to reach the same dimensions at the diagnostics box compared to a period where the positives synch. phases are closer to the magnets, because the transverse envelope is larger near the magnets. The first case will also have larger dimensions inside the magnets, increasing therefore the possible losses.

The choice of the absolute value of the synchronous phases is also very important: keeping the phase advance constant, a larger value would better preserve the longitudinal plane from undesired emittance increase, but this imply again to reduce the operating accelerating field.

Only by simulations is possible to take into account all this issues at the same time, as function of the A/q, the energy and the position along the accelerator.

## 1.4 2006/2008 ALPI customary acceleration

Since January 2006 the shifts has been prepared in advance with the use of beam simulation codes. Only after conditioning and locking all resonators in amplitude and phase it is possible to know the real performances of the QWRs for that specific shift. The cavity performances are strongly dependent on environmental conditions:

1. The maximum $E_{acc}$ depends on how long the conditioning process has lasted. The time available for conditioning depends on how the shifts are scheduled. Therefore the shifts are usually grouped by the number of required cavities, so to exploit the conditioning time for more than a single shift. If the cavities are not in use, their performances decrease and one has to condition them again.

2. The possibility of locking a low-β cavity depends on the stability of the cryogenic system. The system itself becomes stable only once all the required cavities are set to a specific $E_{acc}$ and locked. It could happen that after few hours while the system is running, one discovers that specific cavities have to work at lower field.

3. Sometimes happens that the cavity tuners/couplers can get blocked because of an ice problem. The cavity operation can be recovered only if the entire cryostat is brought to room temperature. Therefore for that specific shift the cavity has to be switched off.

For these reasons in Tab. 1.2 the number of required cavities and the number of cavities out of order for the shifts of 2006/2008. From the comparison of Fig. 1.5(a) with Fig. 1.5(b) one can see that the average of the final energy is stable during the period but the number of required cavities has diminished and the number of the not available cavities has increased. The reason is that most of the cryostats have more than 10 years of operation and some parts easily get broken due to age. Once the cryostat is repaired and the QWRs freshly polished the performances become higher than before.

For the last shift with $^{132}$Xe, for example, 30% of the cavities were switched off because of failures, but the users were nevertheless able to perform their experiments with one of the most demanding beam ever accelerated by ALPI. The reason for this exceptional result is the careful procedure which has been set-up during these years.

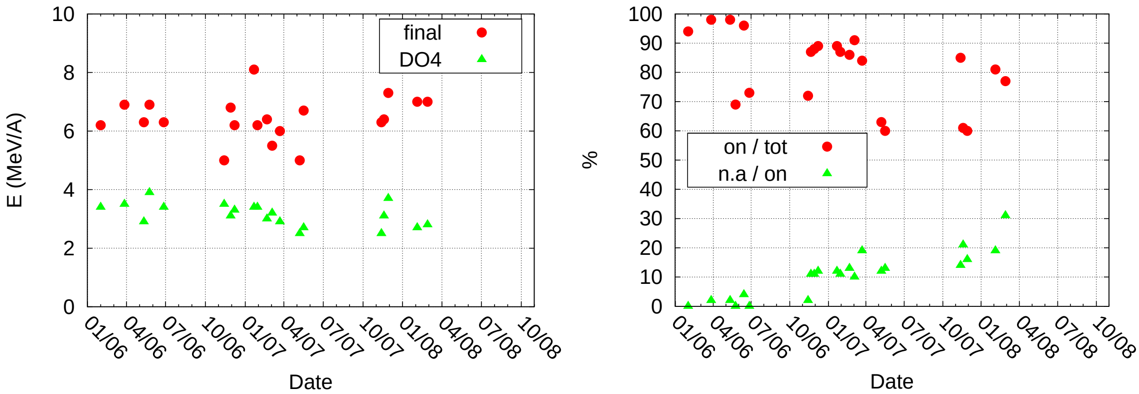


(a) ALPI shifts energies. (b) ALPI shifts cavity usage.

Figure 1.5: ALPI shifts graphical summary.

Table 1.2: Summary of ALPI shifts since January 2006 with the described beam preparation procedure. The energy at DO4 characterizes the stripping option described in Chapter 4.

| yy-mm-dd | Inj. | beam | | | E (MeV/A) | | ALPI cav. | |
|---|---|---|---|---|---|---|---|---|
| | | A | Ion | q | final | D04 | req. | n/a |
| 06-02-01 | T | 82 | Se | 11 | 6.2 | 3.4 | 60 | 0 |
| 06-03-28 | T | 48 | Ca | 9 | 6.9 | 3.5 | 51 | 1 |
| 06-05-12 | T | 120 | Sn | 14 | 6.3 | 2.9 | 63 | 1 |
| 06-05-25 | T | 48 | Ca | 9 | 6.9 | 3.9 | 36 | 0 |
| 06-06-14 | T | 32 | S | 10 | 14.5 | 6.6 | 50 | 2 |
| 06-06-27 | T | 64 | Ni | 11 | 6.3 | 3.4 | 38 | 0 |
| 06-11-14 | T | 82 | Se | 11 | 5.0 | 3.5 | 46 | 1 |
| 06-11-21 | T | 58 | Ni | 4 | 11.3 | 5.4 | 45 | 5 |
| 06-11-29 | P | 22 | Ne | 22 | 6.8 | 3.1 | 56 | 6 |
| 06-12-08 | T | 90 | Zr | 12 | 6.2 | 3.3 | 57 | 7 |
| 07-01-22 | P | 22 | Ne | 4 | 8.1 | 3.4 | 57 | 7 |
| 07-01-30 | T | 82 | Se | 12 | 6.2 | 3.4 | 45 | 5 |
| 07-02-21 | T | 70 | Zn | 10 | 6.4 | 3.0 | 55 | 7 |
| 07-03-05 | P | 136 | Xe | 22 | 5.5 | 3.2 | 58 | 6 |
| 07-03-23 | T | 96 | Zr | 13 | 6.0 | 2.9 | 54 | 10 |
| 07-05-08 | T | 82 | Se | 12 | 5.0 | 2.5 | 33 | 4 |
| 07-05-17 | T | 48 | Ca | 9 | 6.7 | 2.7 | 31 | 4 |
| 07-11-13 | T | 82 | Se | 12 | 6.3 | 2.5 | 44 | 6 |
| 07-11-19 | P | 40 | Ar | 9 | 6.4 | 3.1 | 39 | 8 |
| 07-11-29 | T | 48 | Ca | 9 | 7.3 | 3.7 | 31 | 5 |
| 08-02-04 | P | 136 | Xe | 23 | 7.0 | 2.7 | 52 | 10 |
| 08-02-28 | P | 136 | Xe | 23 | 7.0 | 2.8 | 49 | 15 |

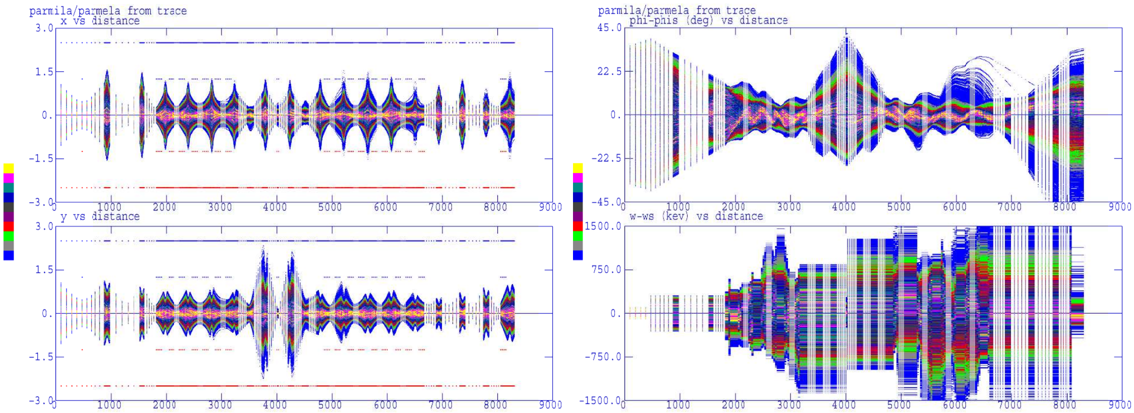


(a) Transverse envelopes. (b) Longitudinal envelopes.

Figure 1.6: Example of acceleration of a Tandem beam ($^{70}Zn^{10+}$).

### 1.4.1 Beam preparation procedure

Once the $E_{acc}$ of ALPI cavities is known, it is possible to start simulating the beam dynamics for that specific shift. First of all a simple computer code, developed on an Excel spreadsheet, sets the preliminary values of the reference phase for each resonator, so as to minimize the average phase width of the bunch and to keep its oscillations under control: this is done, normally, by a proper choice of the phase between the two values -20 and +20. In the particular case of the very first lower $\beta_0$ cavities, lower values of $E_{acc}$ than the available ones need to be input for this purpose.

As a second step, this setup for the longitudinal dynamics is inserted into a Trace 3D [9] sheet, through which the quadrupole gradients are regulated, so as to have a beam which is well enough focused in the cavities and not too large in the magnets. In this step, one has to make sure that the chosen dynamics does not imply quadrupole gradients larger than the available ones. Otherwise one needs to go back to the Excel spreadsheet and change resonators reference phase, thus iterating the process.

The last step is a multi-particle simulation with the code PARMELA [10], through which possible longitudinal beam losses (and their causes) are searched and quadrupole gradients are corrected in order to minimize transverse losses.

Once this series of simulations provides reasonable results, the values of the resonator reference phase, and the quadrupole gradients, are passed to the operation group to be implemented in ALPI for beam transport and acceleration. This procedure was conceived around two years ago and had a significant effect in speeding up the linac setup and reducing beam losses.

The beam simulation operation is fundamental for the proper setting of the accelerator to take into account the correlation between transverse and longitudinal dynamics. The case of the lack of a single cryostat is a clear example, because one needs to minimize the phase width at the following cavity but also to proper focus transversely the beam so to overcome the asymmetry of the defocusing force respect to the center of the period. Also the information of beam emittance is lacking experimentally, because there is no way to perform the correlation between time and energy spread.

For the beams coming from TANDEM, the longitudinal input parameters are $\Delta t$ =1.2 ns (70 deg @ 160 MHz) and $\Delta E/E$ = ±5%, values which have been experimentally confirmed (see Fig. 1.6). The time spread comes from the 5 MHz and 10 MHz pulsing system located between the 1- source and the TANDEM tank and the energy spread from the feedback on the TANDEM voltage tuning. Lower energy spread could be obtained at the cost of a lower current. Next Chapter will cover the description of the input parameters for the beams coming from PIAVE.

### 1.4.2 An example of beam energy measurement: $^{70}Zn^{10+}$

Sometimes the users require an energy measurement to confirm their TOF measurements performed at the experimental apparatus. The beam is normally delivered to users with an accuracy of 1% on the energy measured with the final dipole, if higher accuracy is needed on has to prepare the ALPI high-energy line for the experimental set-up.

The diagnostics boxes D10 and D11 with only the magnetic triplet 3Q15 in between can hold the Fast Faraday Cups (FFC [11]) needed for the TOF measurement. A "cup" FFC was installed in D10 and a "strip line" FFC (SLFFC) in D11. The set-up is sketched in Fig. 1.7.

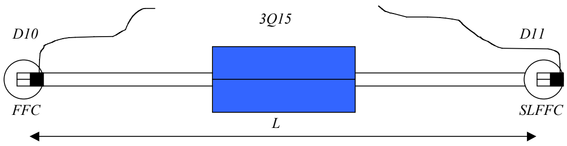


Figure 1.7: Energy measurement set-up.

Despite to the short distance between the two FFCs, the resulting resolution in energy (0.25%) is high enough to exceed the performance of the measurement with the dipoles. In fact the resolution of this procedure is reduced by the uncertainty of the alignment of the reference trajectory in the dipoles with both the upstream line and the diagnostics box (DE2) which follows, in addition to the experimental problem of choosing the center of a beam horizontally broadened by the energy dispersion.

| parameter | value | unit |
|---|---|---|
| $L$ | $4.327 \pm 0.005$ | m |
| $\delta T$ | $2.311 \pm 0.006$ | ns |
| $T_{XTU}$ | $223.73 \pm 0.13$ | ns |
| $T_{exp}$ | $122.79 \pm 0.01$ | ns |

Table 1.3: Experimental set-up parameters and time measurement results for $^{90}Zr^{12+}$.

For the energy measurement performed during the $^{90}Zr^{12+}$ shift, the length of the distance $L$ between the two FFCs was measured directly with an accuracy of 5 mm and the value is listed in Tab. 1.3. The time delay given by the length of the signal cables between FFCs and oscilloscope was measured following the standard open-loop procedure. The difference in time $\delta T$ between the cable of the FFC and the one of the SLFFC is listed in Tab. 1.3. The related error is given by the digital oscilloscope software which compares and averages the rising edge of multiple waves going forth and back.

Once the length and the time delay due to the cables were known, it just remained to measure the distance in time between the two FFCs for the accelerated and non accelerated beam. The ALPI bunching frequency is set to 5 MHz, which means one bunch every 0.2 μs. The results for the XTU-only beam ($T_{XTU}$) and the accelerated beam ($T_{exp}$) are listed in Tab. 1.3, where the errors depend on the sharpness of the bunch edges, related to the bunch length itself.

The energy corresponding to the measured time intervals is calculated via the non-relativistic formula $E = \frac{1}{2}mc^2\beta^2$, with $\beta = \frac{L}{(T+\delta T)c}$.

Regarding the errors, the quadratic propagation has been used and the resulting expression is

$$\Delta E = \sqrt{\left(\frac{\Delta T}{T+\delta T}\right)^2 + \left(\frac{\Delta L}{L}\right)^2}.$$

Table 1.4 shows the final results. The nominal energy for the XTU-only beam is given with a precision of 0.5% by the voltage (13.2 MV) which the machine was set to.

| | nominal E (MeV) | measured E (MeV) |
|---|---|---|
| XTU only | 171.6 ± 0.9 | 171.4 ± 0.4 |
| to experiment | 560 ± 5 | 563.6 ± 1.3 |

Table 1.4: Energy measurement results for $^{90}Zr^{12+}$.

# Bibliography

[1] G. Fortuna and al., "The ALPI project at the Laboratori Nazionali di Legnaro," *Nuclear Instruments and Methods A*, vol. 287, pp. 253–256, November 1990.

[2] A. Dainelli, A. Facco, A. Lombardi, and E. A. Togun, "Beam optics progress for the ALPI project," in *Proceedings of EPAC 1990*, (Nice, France), pp. 1291–1293, 1990.

[3] G. Fortuna and al., "Completion of the first phase and studies for the upgrading of the ALPI project at LNL," in *Proceedings of EPAC 1992*, (Berlin, Germany), pp. 170–172, 1992.

[4] A. M. Porcellato, S. Stark, and al., "Operation experience with ALPI Nb/Cu resonators," in *Proceedings of EPAC 2004*, (Lucerne, Switzerland), pp. 1018–1020, 2004.

[5] S. Stark, A. M. Porcellato, and al., "A novel sputtered medium beta cavity for ALPI," in *Proceedings of 13$^{th}$ International Workshop on RF Superconductivity*, (Peking, China), 2007.

[6] A. Facco and J. S. Sokolowski, "The Low Beta Section of the ALP1 Accelerator," in *Proceedings of EPAC 1994*, (London, England), 1994.

[7] A. Facco and V. Zviagintsev, "Completion of the LNL Bulk Niobium Low Beta Quarter Wave Resonators," in *Proceedings of the 9$^{th}$ Workshop on RF Superconductivity*, (Santa Fe (NM), USA), 1999.

[8] P. Modanese, A. Beltramin, L. Bertazzo, A. Calore, T. Contran, A. Dainelli, F. Poletto, and A. M. Porcellato, "Upgrading of ALPI-LINAC cryogenic transfer lines," in *LNL Annual Report 2006*, (Legnaro, Italy), pp. 157–158, INFN, 2006.

[9] K. R. Crandall and D. P. Rusthoi, "Trace 3-D," tech. rep.

[10] L. M. Young and J. H. Billen, "PARMELA Version 3," tech. rep.

[11] M. Bellato, A. Dainelli, and M. Poggi, "Bunch length measurements in the ALPI linac at LNL," *Nuclear Instruments and Methods A*, vol. 382, pp. 118–120, November 1996.